Semiconductors, Vol. 37, No. 2, 2003, pp. 124–130. Translated from Fizika i Tekhnika Poluprovodnikov, Vol. 37, No. 2, 2003, pp. 134–141.

ATOMIC STRUCTURE AND NONELECTRONIC PROPERTIES OF SEMICONDUCTORS

Self-Organization of Laser-Induced Point Defects at the Initial Stages of Inelastic Photodeformation in Germanium

S. V. Vintsents*, A. V. Zaitseva, and G. S. Plotnikov****

** Institute of Radio Engineering and Electronics, Russian Academy of Sciences (Fryazino Branch), pl. Vvedenskogo 1, Fryazino, Moscow oblast, 141120 Russia*

e-mail: alkeev@ms.ire.rssi.ru

*** Faculty of Physics, Moscow State University, Vorob'evy gory, Moscow, 119899 Russia*

Submitted June 13, 2002; accepted for publication June 18, 2002

Abstract—Atomic-force microscopy is applied to study the characteristic features of the relief forming on a germanium surface at the initial stages of multiple laser-induced deformation. Both elastic and inelastic strains can be induced in a semiconductor surface layer irradiated by scanning laser pulses. It is shown that the elastic deformation of the Ge surface does not affect its initial nanorelief, whereas inelastic deformation initiates a low-threshold formation of ordered nanostructures on the surface. Correlation between this phenomenon and the laser-induced generation of point defects near the inelastic-strain threshold is considered.

INTRODUCTION

One of the most interesting phenomena induced by pulsed laser irradiation of solids is the appearance of strain and the related displacement of the surface layers [1, 2]. In conditions of multiple local irradiation of metals and semiconductors, nondestructive (elastic) shear strain $\varphi = dU_z/dr$ (where r is the coordinate along the laser beam radius) corresponds to effective normal surface displacements U_z on the order of subnanometers [3, 4]. Irradiation in the nanosecond mode ($\tau \leq$ 1–100 ns) has been studied in detail because of acoustic [5, 6] and other fast processes that take place, for example, during the laser annealing of defects [7, 8].

Slower quasi-static ("photothermal", [9]) strain appears under single-mode irradiations, with the typical size of the light spot on the surface $\omega \approx$ 10–100 μm and the exposure time $\tau \geq$ 0.1–1.0 μs [10, 11]. Such quasi-static strain (if it is elastic or quasi-elastic), holds promise for the contactless local monitoring of thermal [12] and optical [13] parameters of surface layers, for studying the kinetics of the first-order phase transition in thin semiconductor films [14, 15], as well as the revealing and 3D analysis of special modes in the kinetics of local nondestructive surface displacement [10, 11]. Usually, a typical relaxation time of the discussed strain t ranges from 1 to 100 μs [3, 4].

During the development of pulsed photoinduced quasi-static strain in semiconductors (and metals), different channels of defect formation may be activated. Three main factors have traditionally been considered as those governing laser-induced defect formation in semiconductors: heating, energy transfer from photoexcited carriers to defects, and strain of the surface layer itself [16–19]. According to the electron-strain-thermal (ESH) theory of defect formation [16, 19] the processes of point defect formation prevail until the photoinduced heating is "below-threshold" (does not result in the short-term melting of the surface layers [7, 8]).

It was shown in previous studies [3, 20–22] that, in the conditions of multiple local irradiation of semiconductors, the elastic form of strain gives way to the inelastic one even at low shear strains, $10^{-5} < \varphi_0(W_0) < 10^{-4}$, where $W_0 \leq 0.1$ [J/cm^2] is the threshold energy density of submicrosecond laser pulses. It was also shown that, at least at the initial stages of inelastic deformation (with a moderate number of pulses $N \leq 10^3$), the amplitude of temperature inhomogenities over the surface reaches only a few tens of degrees. Under these conditions, the multiple deformation of semiconductor local regions (within a size of $\approx 2\omega$) may give rise to the so-called size effects [3, 20, 21] and enhance the influence of strain on the generation (and redistribution) of point defects [22–24].

The slow electron states (of fluctuation origin) in a thin insulating GeO_2 film [23] and the vacancies that are driven from the interface into the bulk [24] may be considered among the defects that are sensitive to the threshold $\varphi_0(W_0)$ in germanium. Note that the previously described [23, 24] contribution from the generation and accumulation of defects to changes in the relief on an actual Ge surface subjected to cyclic inelastic deformation has not yet been detected in experiments.

For the direct investigation of the initial stages of inelastic strain in germanium and the detection of corresponding residual displacements ΔU_zon a nanometer scale, we used atomic-force microscopy (AFM) to study the nanorelief produced on a germanium surface

1063-7826/03/3701-0124$24.00 © 2003 MAIK "Nauka/Interperiodica"

subjected to scanning pulsed laser irradiation ($N \le 10^3$) in the vicinity of previously determined [3, 22–24] deformation thresholds $\varphi_0(W_0)$.

EXPERIMENTAL

Similar to [23, 24], the (111) surfaces of high-resistivity (ρ = 25–30 Ω cm) *n*-Ge:Sb single crystals etched in H^2O^2 were scanned by laser pulses in air at room temperature. A normal-incidence laser beam with λ = 0.53 μm was used for the scanning method, which is similar to that described in [22–24]: the repetition rate was $f \approx 10^4$ s^{-1}; a typical pulse duration was $\tau \approx 0.4$–0.5 μs; the single-mode laser beam produced a Gaussian spot with a size of $2\omega \approx 70$ μm on the surface; the velocity and the step of scanning were $v \approx 1$–5 mm/s and $\delta \approx 5$–10 μm, respectively.

Our method of overlapping the laser spots on the surface allowed us to obtain a spread no greater than 5–7% in the maximal incident-energy density W within each scanned area of $\approx 3 \times 5$ mm^2. Note that W[mJ/cm^2] = $E/\pi\omega^2$, where E is the measured total energy of the pulse [22–24]. The single-mode character of the laser beam should be emphasized: the dependence of the intensity of light on the radial coordinate r and time t (as in [10, 11, 20]) can be closely approximated by the formula $I(r, t) = W\exp(-r^2/\omega^2)(t/\tau^2)\exp(-t/\tau)$.

We considered the energy densities W in the range from 0 to 150 mJ/cm^2, which includes the previously determined inelastic-strain thresholds in germanium [3, 23, 24] $W_0 \approx$ 65–70 mJ/cm^2 and is essentially below the W_m values predicted for the melting thresholds upon long-term (submicrosecond) irradiation: $W_m \ge$ (1.2–1.5) J/cm^2 [7, 8].

Profiles of the surface nanorelief were measured and the topology of the surface was studied on a submicron scale with the use of a Nanoscope-111a-type atomic-force microscope (AFM) (Digital Instruments), which operated in air in the contact mode. Levers with a rigidity of $\approx$0.01–0.2 N/m provided a nondestructive mode for studying the relief on the Ge surface. Images of the surface regions after exposure to the scanning laser pulses were processed using specialized "FemtoScan-001" software [25].

RESULTS

Figure 1 shows the results of the AFM study of the actual germanium surface (*1*) before and after laser irradiation with W = (*2*) 50, (*3*) 85, (*4*) 110, (*2*), and (*5*) 150 mJ/cm^2. According to our measurements, the average difference in height in the relief of the initial (unirradiated) surface is no larger than $\delta U_z \le$ 2–5 nm (Fig. 1, *1*). In some areas, we observe scratches as deep as 10 nm, which apparently are traces from the mechanical grinding and remained after the chemical etching of the surface.

The situation is nearly the same in the region irradiated with W = 50 mJ/cm^2 (Fig. 1, *2*): the amplitudes of the random nanorelief δU_z remain as before and neither laser-induced residual strain nor additional displacement of the surface is revealed. This circumstance correlates with the data obtained previously [3, 23, 24] for the elastic mode of laser-induced deformation of Ge surface layers at $W < W_0$ = 65–70 mJ/cm^2. It is noteworthy that previous studies [23, 24] revealed an enhanced formation of point defects at the inelastic-strain thresholds $\varphi_0(W_0)$.

At the initial stages ($N \le 10^3$) of inelastic laser-induced strain ($W \ge 85$ mJ/cm$^2 \approx 1.2W_0$), it was only in separated uncoordinated surface spots (Fig. 1, *3*) with a diameter of several micrometers and a total area accounting for 5–10% of the scanned surface area that we observed the appearance of a threshold (with respect to W) for formation of nonoriented clusters (Fig. 2, *1*) and for self-organization of laser-induced point defects [22–24] into two-dimensional (2D) arrays of surface nanorelief (Fig. 2, *2*) with the amplitude of irreversible normal surface displacements $\delta U_z \approx$ 10–20 nm (Fig. 2, *3*). The size of nonoriented clusters was on the order of $\approx$100 nm and the spacings in the emerging 2D array $a \approx$ 550–600 nm (perpendicular to the direction of scanning) and $b \approx$ 350–400 nm (along the crystallographic directions of [100] type (Fig. 2)). Note that these values are considerably smaller than the laser spot size $\approx 2\omega$ and the scanning pitch δ (see above).

The presence of regions with a weak plastic strain in Fig. 1, *3* and the clearly defined horizontal sections (so-called "plateaus") in Fig. 2, *3* allows us to set a reference point along the z direction (normal to the surface) with an accuracy of $\approx \delta U_z/2$; in other words, we determined the zero level of the initial surface. As a result, regular elevations of nanorelief appearing in 2D submicron arrays are attributed to the transfer of material from well-developed circumferential "nanotrenches" around each of the "nanohills".

The stable formation of ordered (periodic) structures over the entire area of the irradiated surface is observed at an energy density $W \ge 110$ mJ/cm$^2 \approx 1.5$–$1.6W_0$. When W is much higher than W_0, separate hills merge into parallel ridges (Fig. 1, *4*), i. e., the 2D arrays give way to one-dimensional structures with a period $\approx a$ and a height difference $\Delta U_z \approx$ 20–40 nm.

Irradiation of the germanium surface with $W \ge$ 150 mJ/cm$^2 \approx 2.2$–$2.5W_0$ results in an essentially more complicated pattern of microplastic strain. For example, simultaneously with the growth of the amplitudes of irreversible displacements ΔU_z to 30–60 nm in the submicrometer arrays, we observed an additional generation of structures with a large (several micrometers) spatial period (Fig. 1, *5*). With a further increase in W, the evolution of multiple inelastic laser-induced strains in the germanium surface layer had mainly a destruc-

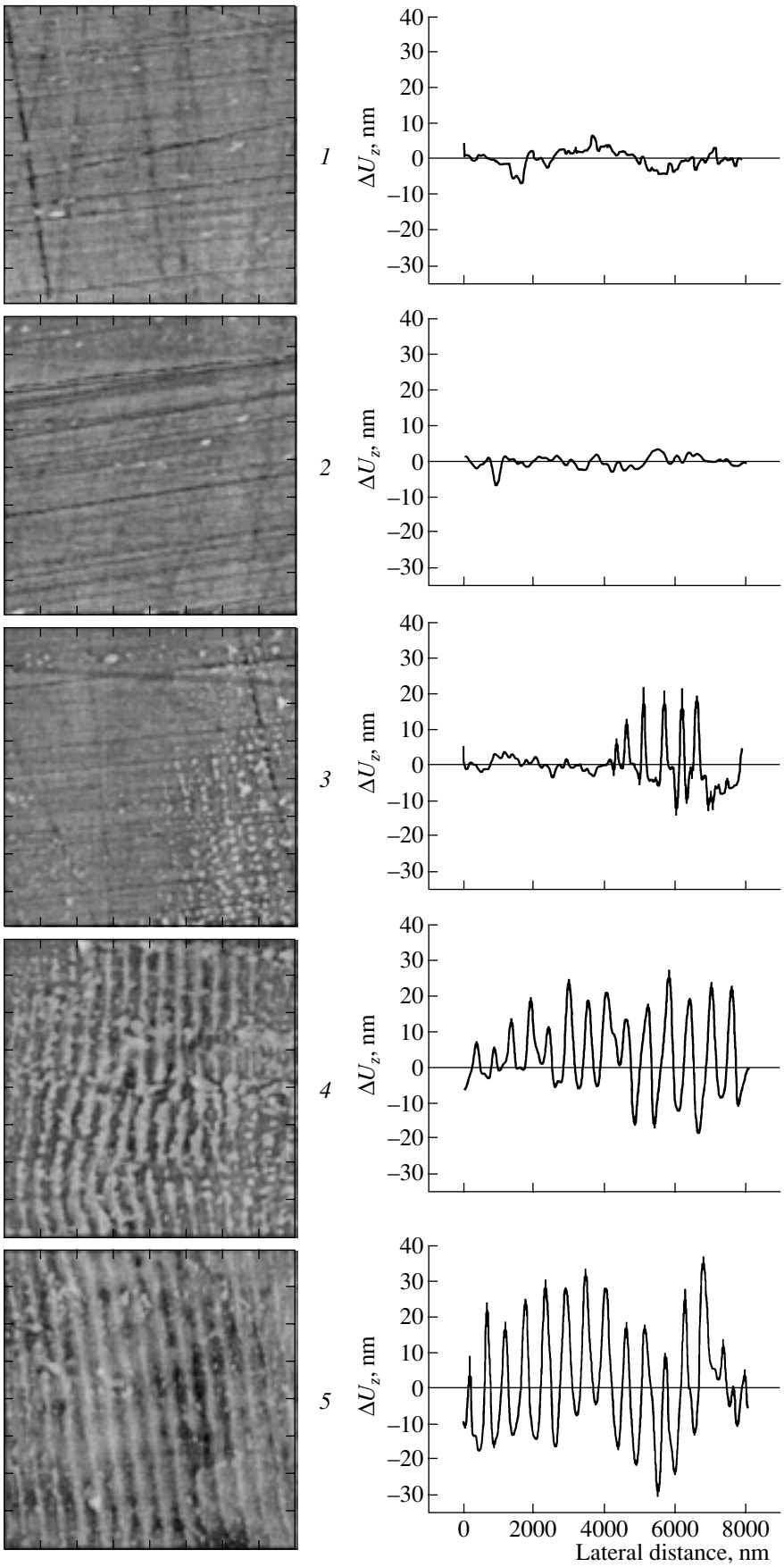
1
2
3
4
5
ΔU_z, nm
40
30
20
10
0
–10
–20
–30
0
2000
4000
6000
8000
Lateral distance, nm

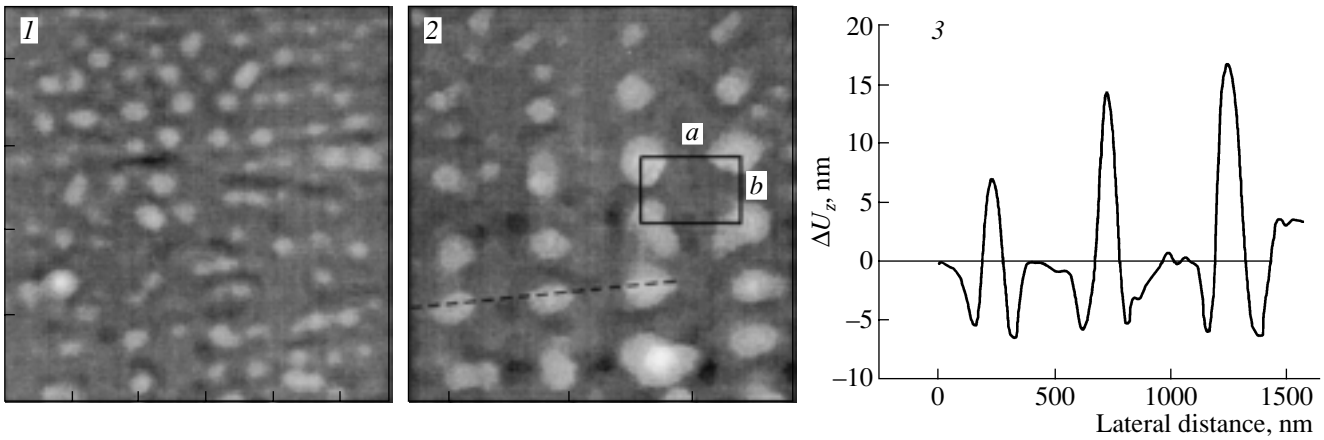

Fig. 2. AFM images at the initial stages of the formation of (*1*) nonoriented clusters and (*2*) 2D gratings; (*3*) vertical profiles of irreversible displacements ΔU_z at the germanium surface subjected to inelastic deformation near the thresholds $W_1 \approx 1.2$–$1.5W_0$. The size of images *1* and *2* is 2300×2300 nm^2.

tive character and fell outside the scope of this AFM study.

DISCUSSION

In what follows, we provide an interpretation of the most important results and present a number of estimates. Let us recall that the modes of multipulse local irradiation of semiconductors and metals have traditionally been divided (see, e. g., [3, 20–24] and references therein) into destructive ($W > W_d$) and nondestructive ($W < W_0$). The upper damage threshold W_d is usually defined by the onset of the formation of extended (on the order of micrometers) damaged sites, which are visible under a microscope, or by a pronounced drop in the mirror reflectivity of the scanning beam from the surface [3, 10, 26–29]. These final stages of degradation with the appearance of microcracks can be detected with the use of acoustic waves, among other methods [30, 31].

A detailed study of the changes induced at the initial stages of irradiation was performed by Vintsents et al. [20–24]. The corresponding lower thresholds W_0, below which no damage is produced on the solid surface even after exposure to a large number of focused laser pulses $N \geq 10^7$–10^9 [3, 4, 10–15], were determined. For the case $N \leq 10^3$, highly sensitive techniques were used: quasi-equilibrium field effect [23], molecular luminescence probes [24], photothermal deformation of the surface [20–24], as well as Raman (and diffuse) scattering of light [22, 24] are examples. As a result, it was established that the thresholds W_0 corresponding to the buildup of inelastic strain in Ge surface layers and changes related to the size effect [3, 20] should appear under the surface even at the earliest stages of irradiation [21]. With a further increase in W above W_0, a threshold growth of the concentration of defects was detected both in the thin GeO_2 oxide film [23] and in the deeper layers in the bulk of the material [24]. Similar low-threshold phenomena were also observed in Si and GaAs samples [22].

Thus, one might expect that the laser irradiation of solids at $W_0 \leq W \leq W_d$ in the inelastic mode of multiple local strain is mostly destructive. However, this statement appears to be true only for large N [3, 22]. The results of AFM studies (Figs. 1, 2) indicate the exact opposite situation at $N \leq 10^3$: at the initial stage of inelastic deformation, laser-induced point defects [22–24] are self-organized into periodic nanostructures on the germanium surface. In this case, the discussed energy interval may be considered as the range of controlled inelastic effects where, along with W, the governing parameters can also be N, ω, τ, and λ.

Periodic surface structures appearing as a result of the irradiation of solids have already been observed. The most thoroughly studied case is the formation of a surface periodic relief due to the instability that develops as a result of interference between incident and diffracted (surface) electromagnetic waves. The spatial orientation of such interference gratings (IG) should depend on the polarization and the angle of incidence of radiation, while their period strictly correlates with the wavelength and is proportional to λ [32–34].

In this study, the orientation of the observed gratings is defined mainly by the crystallographic symmetry (Fig. 2, *2*) or by the direction of scanning (Fig. 1, *5*). At normal incidence of the beam, the resulting structures had different periods (*a* and *b*), which were not closely

Fig. 1. AFM images and nanorelief profiles of the actual germanium surface irradiated with multiple ($N \leq 10^3$) laser pulses of submicrosecond duration for different energy densities W: (*1*) unirradiated sample, $W =$ (*2*) 50, (*3*) 85, (*4*) 110, and (*5*) 150 mJ/cm^2. The size of images is 8×8 μm^2. Plots to the right show the displacement of surface ΔU_z along the vertical section of sample.

related to λ, ω, or δ (see above). The formation of gratings has a pronounced low-threshold character and takes place only within the energy range $W \geq W_1 \approx (1.2–1.5)W_0 < W_d \ll W_m$.

In this context, we believe that, at the initial stages (at $N \leq 10^3$) of inelastic ($W > W_0$) light-induced strain, i. e., far from the damage thresholds W_d [22, 26–29] and the calculated melting thresholds W_m [7, 8] the defect-diffusion microplasticity mechanism [36] (unrelated to dislocations [35]) is realized on the solid germanium surface. It is only in the inelastic mode of deformation that critical concentrations of defects can be attained due to the successive (from pulse to pulse) accumulation of laser-induced point defects [37] and the appreciable enhancement of this process at the strain thresholds $\varphi_0(W_0)$ [22–24]. According to the theory developed in [38], an increase in the concentration of defects above certain critical values initiates the transition of a system of laser-induced point defects to a spatially inhomogeneous state with a lower energy due to the formation of the so-called defect-deformation (DD) surface structures [38, 39].

According to the present theoretical view [38], generation of DD structures stems from the development of the so-called generation-diffusion-deformation instability (GDDI). This instability can be related to defect–deformation interaction [40, 41], at which the generation or annihilation of defects implies a change in the volume (and the energy) of a crystal and an initial fluctuation of strain gives rise to deformation-induced defect fluxes and/or leads to modulation of their generation rate [38]. As a result, the inhomogeneous field of the defect concentration $n_d(r, t)$ produces forces that are proportional to the concentration gradients and increase the strain in a material. These forces enlarge the initial fluctuation up to the formation of autolocalized defect clusters (Fig. 2). At the early stages of self-organization (Fig. 2, *1*; Fig. 2, *2*), an angular selection of gratings [42, 43] occurs and the AFM-detected changes in the height of the nanorelief (Fig. 2, *3*) can be interpreted in terms of the theory of 2D gratings [38] as clusters of excess atoms in interstices (or as vacancy clusters).

Thus, the initial stages of inelastic deformation in germanium are characterized by generation of both vacancies [24] and interstitial defects, which then organize into small-scale (submicrometer) convex–concave DD structures. The rate of generation of these and some other [23] point defects under the submicrosecond irradiation of semiconductors is still low compared to nanosecond irradiation [7, 8]. We believe that these conditions provide for the realization of a special case of GDDI, i. e., a diffusion–deformation instability (DDI) [38]. The submicrometer (or micrometer) period d of such diffusion–deformation gratings is proportional to the thickness h of the defect-enriched surface region rather than to λ [38]. This circumstance indicates that the arising inhomogeneities in the concentration of defects are indeed fairly small-scale, $d \approx h$ [38], and are mainly due to deformation-induced defect fluxes, while spatial variations in the rate of defect generation or some other mechanisms (for example, the development of microcracks) [44] play only a secondary role in the conditions under consideration.

As was mentioned above, the combined effect of radiation-induced heating, transfert of the electron excitation energy to defects, and deformation of the surface layers causes the efficient formation of point defects under a uniform irradiation of the surface [16, 19]. In the conditions of local multiple irradiation, the effect of strain may become enhanced and, thus, give rise to "size" effects at the thresholds when W_0 values are proportional to ω [3, 20, 21]. In our opinion, this situation enables the low-threshold self-organization of defects into DD gratings at temperatures which are considerably below the melting point.

Indeed, the calculated laser-induced heating of a surface at the thresholds W_0 is still only moderate: $\Delta T_{max} < 100$°C [3, 21, 22]; therefore, the thermal (quenching) mechanism [45] seems to be of minor significance for the pulse-to-pulse accumulation of vacancies (and other defects) at small N. However, in the conditions of appreciably greater N and $W > W_0$, additional heat release is possible due to the action of external forces (associated with the temperature gradients arising from thermal extension [10, 21]) during the accumulation of irreversible displacements of atoms [36].

At small N and $W \approx W_0$, our estimate of d from the length h of the low-temperature diffusion of defects produced near the surface into the bulk of the material (Ge, Si) in terms of the deformation-induced "vacancy pump" [36] is in good agreement with the predictions of theory [38].

When the alternating-sign contact loading of semiconductors is characterized by an asymmetric cycle (i. e., the extension strain exceeds the compression strain in every cycle), the role of vacancy sources is known to dominate over that of sinks [36]. In this case, the kinetics of escape of vacancies to the bulk sinks during compression lags behind the process of their escape from the surface during extension. A "hill" usually forms on semiconductor (or metal) surfaces subjected to local pulsed irradiation [3, 4, 10–13, 20, 21, 23]; i. e., quasi-static deformation in the surface layers of solids is mainly realized in the form of extension, and tensile (and shear) stresses are dominant. According to the vacancy-pump model [36], the thickness of the defect-enriched layer h (and the diffusion length) should be defined by the total time $N\tau_{1/2}$ of the stressed state of a semiconductor.

In the case of germanium, the half-time of relaxation of the photoinduced stresses $\tau_{1/2} \approx 10–15$ μs starting from the leading edge of each pulse (for every beam size 2ω, the time $\tau_{1/2}$ is different [10, 11]) can be estimated from the experiments with the kinetics of local quasi-static photoinduced strain [46] or from the instantaneous profiles of the surface displacements

[47]. As determined in [36], largest values $h_{max} \approx 2(D_v N\tau_{1/2})^{1/2} = 420$ nm, where $D_v \approx 4.3 \times 10^{-8}$ cm^2/s is the diffusion coefficient of vacancies in germanium extrapolated to room temperature ($D_v \approx 10^{-4}\exp(-0.2/kT)$ [48]) and $N \sim 10^3$ is the maximal number of photodeformation pulses used during the scanning irradiation.

Close correlation between the estimates $h \approx 420$ nm and the grating periods obtained in experiment, $d \approx$ 350–550 nm (*a* and *b* sections in Fig. 2, *2*), may be considered as further verification of the defect–deformation mechanism [38] for the formation of residual nanometer displacements ΔU_zat the initial stages of inelastic photoinduced deformation in germanium. A significant role in this process is apparently played by the point-defect generation (discovered previously [23, 24] at the deformation thresholds $\varphi_0(W_0)$) in the surface layer and at the Ge–GeO_2 interfaces. The maximal amplitudes $\delta U_z \approx$ 30–60 nm in Fig. 1, *5* are also in good agreement with the estimate $\Delta U_z \equiv \xi_q \approx h/10 \approx 40$ nm obtained for the stationary state of gratings, i. e., after the completion of angle selection and the monochromatization of their spectrum [38].

In conclusion, we should note the 2D character of the structures generated near the thresholds of the grating formation $W_1 \approx 1.2$–$1.5W_0$ (Fig. 2, *2*) and their nonuniform distribution over the surface; in our opinion, the separate "spots" of generation may be interpreted as sites with an enhanced concentration of biographical defects in germanium (Fig. 1, *3*). In such regions, which, at first, are undistinguishable, the critical concentrations of point defects should be most readily attained under irradiation. This finding may be of use in revealing and outlining defect regions. At a considerable excess over the thresholds W_1, the inelastic photoinduced strain features a more uniform distribution over the surface; however, its identification becomes a challenge because of the additional generation of other structures with a larger period (Fig. 1, *5*). The possible influence of the direction of scanning on the merging of hills into ridges on the surface (Fig. 1, *4*) presents a topic for further investigation. In this context, we are pinning much hope on the future AFM study of semiconductors under local ($\omega \approx$ 10–100 μm) inelastic ($W > W_0$) laser-induced deformation for a different number of pulses *N* when the position of a beam on the surface is fixed.

CONCLUSION

For the first time, we studied experimentally the formation of residual displacements ΔU_z on an actual germanium surface at the initial stages of inelastic quasistatic deformation induced in micrometer-sized ($\omega \leq$ 10–100 μm) surface regions. It is shown that, at a fixed number of pulses, $N \leq 10^3$, in the nondestructive (elastic) photodeformation range (i. e., at $W < W_0$), no effective accumulation of defects occurs and the surface relief remains random. At the very beginning of microplastic changes, at $W_0 < W < 1.2$–$1.5W_0$, an intense [23, 24] concealed (i. e., subsurface, latent) accumulation of point defects with a quasi-uniform distribution of their concentration over the surface prevails over the main part of the scanned area. As the microplastic strain increases (at $W \geq W_1 \approx (1.2$–$1.5W_0)$) we observe the low-threshold self-organization of light-induced defects [23, 24] into deformation–defect "convex-concave" nanostructures, which can be adequately explained in terms of existing theory [38]. The discovered mechanism for the formation of regular residual displacements of nanometer size ΔU_z directly points to the defect–diffusion (unrelated to dislocations [35]) character of microplasticity in the germanium surface layers [36] irradiated by multiple laser pulses in the temperature range near the brittle point.

ACKNOWLEDGMENTS

We are grateful to V. B. Zaitsev for his useful comments.

REFERENCES

1. V. É. Gusev and A. A. Karabutov, *Laser Optical Acoustics* (Nauka, Moscow, 1991).
2. V. P. Zharov and V. S. Letokhov, *Laser Optical–Acoustic Spectroscopy* (Nauka, Moscow, 1984).
3. A. G. Barskov and S. V. Vintsents, Fiz. Tverd. Tela **36**, 2590 (1994) [Phys. Solid State **36**, 1411 (1994)].
4. S. V. Vintsents and S. G. Dmitriev, Zh. Tekh. Fiz. **67** (2), 105 (1997) [Tech. Phys. **42**, 216 (1997)].
5. S. A. Akhmanov and V. É. Gusev, Usp. Fiz. Nauk **162** (3), 3 (1992) [Sov. Phys.–Usp. **35**, 153 (1992)].
6. L. M. Lyamshev, *Laser Thermoacoustic Generation of Sound* (Nauka, Moscow, 1989).
7. R. F. Wood, C. W. White, and R. T. Young, Semicond. Semimet. **23** (1984).
8. A. V. Dvurechenskiĭ, G. A. Kachurin, E. V. Nidaev, and L. S. Smirnov, *Pulsed Annealing of Semiconductor Materials* (Nauka, Moscow, 1982).
9. *Proceedings of 8th International ??Topical Meeting on Photoacoustic and Photothermal Phenomena* (Paris, 1994).
10. S. V. Vintsents, S. G. Dmitriev, and O. G. Shagimuratov, Fiz. Tverd. Tela **38**, 993 (1996) [Phys. Solid State **38**, 552 (1996)].
11. S. V. Vintsents, S. G. Dmitriev, and K. I. Spiridonov, Fiz. Tverd. Tela **39**, 2224 (1997) [Phys. Solid State **39**, 1985 (1997)].
12. S. V. Vintsents and V. B. Sandomirskii, Phys. Status Solidi A **133**, K7 (1992).
13. S. V. Vintsents, V. I. Mirgorodskiĭ, and Sh. S. Khalilov, Poverkhnost **9**, 157 (1990).
14. S. V. Vintsents, V. F. Kiselev, N. L. Levshin, and V. B. Sandomirsky, Surf. Sci. **241**, 225 (1991).
15. S. V. Vintsents and N. L. Levshin, Poverkhnost **2**, 67 (1993).
16. V. I. Emel'yanov and P. K. Kashkarov, Poverkhnost **2**, 77 (1990).

17. P. K. Kashkarov and V. F. Kiselev, Izv. Akad. Nauk SSSR, Ser. Fiz. **50** (3), 435 (1986).
18. V. A. Zuev, V. G. Litovchenko, G. A. Sukach, and N. M. Torchun, Ukr. Fiz. Zh. **21** (5), 752 (1976).
19. V. I. Emel'yanov and P. K. Kashkarov, Appl. Phys. A **55**, 161 (1992).
20. S. V. Vintsents and S. G. Dmitriev, Pis'ma Zh. Tekh. Fiz. **21** (19), 1 (1995) [JTP Lett. **21**, 767 (1995)].
21. S. V. Vintsents, S. G. Dmitriev, and O. G. Shagimuratov, Pis'ma Zh. Tekh. Fiz. **22** (8), 8 (1996) [JTP Lett. **22**, 602 (1996)].
22. S. V. Vintsents, A. V. Zoteev, and G. S. Plotnikov, Fiz. Tekh. Poluprovodn. (St. Petersburg) **36**, 902 (2002) [Semiconductors **36**, 841 (2002)].
23. S. V. Vintsents, S. G. Dmitriev, R. A. Zakharov, and G. S. Plotnikov, Fiz. Tekh. Poluprovodn. (St. Petersburg) **31**, 513 (1997) [Semiconductors **31**, 433 (1997)].
24. S. V. Vintsents, V. B. Zaĭtsev, A. V. Zoteev, *et al.*, Fiz. Tekh. Poluprovodn. (St. Petersburg) **36**, 947 (2002) [Semiconductors **36**, 883 (2002)].
25. A. S. Filonov and I. V. Yaminskiĭ, *User Manual for the Application Package Designed to Control a Sounding Microscope and Processing Images FemtoScan-001* (TsPT, Moscow, 1999).
26. C. S. Lee, N. Koumvakalis, and M. Bass, Appl. Phys. Lett. **47**, 625 (1982); Opt. Eng. **22**, 419 (1983).
27. S. S. Cohen, J. B. Bernstein, and P. W. Wyatt, J. Appl. Phys. **71**, 630 (1992).
28. P. M. Fauchet, Phys. Lett. A **93**, 155 (1993).
29. A. G. Barskov, S. V. Vintsents, G. G. Dvoryankina, *et al.*, Poverkhnost **3**, 79 (1995).
30. V. P. Veĭko, G. V. Dreĭden, Yu. N. Ostrovskiĭ, *et al.*, Zh. Tekh. Fiz. **60** (4), 162 (1990) [Sov. Phys. Tech. Phys. **35**, 499 (1990)].
31. I. A. Konovalov, K. S. Sklyarenko, and S. K. Sklyarenko, Pis'ma Zh. Tekh. Fiz. **20** (6), 26 (1994) [JTP Lett. **20**, 440 (1994)].
32. A. M. Bonch-Bruevich, A. M. Kochengina, M. N. Libenson, *et al.*, Izv. Akad. Nauk SSSR, Ser. Fiz. **46**, 1186 (1982).
33. J. E. Sipe, J. F. Young, J. S. Preston, and H. M. van Driel, Phys. Rev. B **27**, 1141 (1983); Phys. Rev. B **27**, 1155 (1983).
34. S. A. Akhmanov, V. I. Emel'yanov, N. I. Koroteev, and V. N. Seminogov, Usp. Fiz. Nauk **147**, 675 (1985) [Sov. Phys.–Usp. **28**, 1084 (1985)].
35. Yu. I. Golovin and A. I. Tyurin, Fiz. Tverd. Tela **42**, 1818 (2000) [Phys. Solid State **42**, 1865 (2000)].
36. V. P. Alekhin, *Physics of Strength and Plasticity of Surface Layers of Materials* (Nauka, Moscow, 1983).
37. B. L. Volodin, V. I. Emel'yanov, and Yu. G. Shlykov, Kvantovaya Élektron. (Moscow) **20** (1), 57 (1993).
38. V. I. Emel'yanov, Kvantovaya Élektron. (Moscow) **28** (1), 2 (1999).
39. V. I. Emel'yanov, P. K. Kashkarov, N. G. Chechenin, and T. Ditrikh, Fiz. Tverd. Tela **30**, 2259 (1988) [Sov. Phys. Solid State **30**, 1304 (1988)].
40. J. D. Eshelby, Solid State Phys. **3**, 79 (1956).
41. V. S. Vavilov, A. E. Kiv, and O. R. Niyazova, *The Mechanisms of Defect Formation and Migration in Semiconductors* (Nauka, Moscow, 1981).
42. V. P. Veĭko, I. A. Dorofeev, Ya. A. Imas, *et al.*, Pis'ma Zh. Tekh. Fiz. **10**, 15 (1984) [JTP Lett. **10**, 6 (1984)].
43. V. P. Veĭko, Ya. A. Imas, M. N. Libenson, *et al.*, Izv. Akad. Nauk SSSR, Ser. Fiz. **49**, 1236 (1985).
44. F. Kh. Mirzoev, V. Ya. Panchenko, and L. A. Shelepin, Usp. Fiz. Nauk **166** (1), 3 (1996) [Phys.–Usp. **39**, 1 (1996)].
45. N. V. Karlov, N. A. Kirichenko, and B. S. Luk'yanchuk, *Laser Thermochemistry* (Nauka, Moscow, 1992), Chap. 15.
46. S. V. Vintsents and V. I. Mirgorodskiĭ, in *Proceedings of IX All-Union Symposium on Electron Processes on Surface and in Thin Layers of Semiconductors* (Novosibirsk, 1988), Chap. 1, p. 87.
47. S. V. Vintsents, in *Technical Digest of XVI International Conference on Coherent and Nonlinear Optics* (Moscow, 1998), WM 23.
48. V. V. Voronkov, G. I. Voronkova, and M. I. Iglitsin, Fiz. Tekh. Poluprovodn. (Leningrad) **6**, 20 (1972) [Sov. Phys. Semicond. **6**, 14 (1972)].

Translated by A. Sidorova

SPELL: transfert